

Spectral properties of hyperbolic nano-networks with tunable aggregation of simplexes

Marija Mitrović Dankulov^{2,1}, Bosiljka Tadić^{1,3}, Roderick Melnik^{4,5}

¹*Department of Theoretical Physics, Jožef Stefan Institute, Jamova 39, Ljubljana, Slovenia*

²*Scientific Computing Laboratory, Center for the Study of Complex Systems, Institute of Physics Belgrade, University of Belgrade, Pregrevica 118, 11080 Belgrade, Serbia*

³*Complexity Science Hub Vienna, Josephstaderstrasse 39, Vienna, Austria*

⁴*MS2Discovery Interdisciplinary Research Institute; M2NeT Laboratory and Department of Mathematics, Wilfrid Laurier University, 75 University Ave W, Waterloo, ON, Canada N2L 3C5 and*

⁵*BCAM - Basque Center for Applied Mathematics; Alameda de Mazarredo 14, E-48009 Bilbao, Spain*

Cooperative self-assembly can result in complex nano-networks with new hyperbolic geometry. However, the relation between the hyperbolicity and spectral and dynamical features of these structures remains unclear. Using the model of aggregation of simplexes introduced in I [Sci. Rep., 8:1987, 2018], here we study topological and spectral properties of a large class of self-assembled structures consisting of monodisperse building blocks (cliques of size $n = 3, 4, 5, 6$) which self-assemble via sharing the geometrical shapes of a lower order. The size of the shared sub-structure is tuned by varying the chemical affinity ν such that for significant positive ν sharing the largest face is the most probable, while for $\nu < 0$, attaching via a single node dominates. Our results reveal that, while the parameter of hyperbolicity remains $\delta_{max} = 1$ across the assemblies, their structure and spectral dimension d_s vary with the size of cliques n and the affinity when $\nu \geq 0$. In this range, we find that $d_s > 4$ can be reached for $n \geq 5$ and sufficiently large ν . For the aggregates of triangles and tetrahedra, the spectral dimension remains in the range $d_s \in [2, 4)$, as well as for the higher cliques at vanishing affinity. On the other end, for $\nu < 0$, we find $d_s \approx 1.57$ independently on n . Moreover, the spectral distribution of the normalised Laplacian eigenvalues has a characteristic shape with peaks and a pronounced minimum, representing the hierarchical architecture of the simplicial complexes. These findings show how the structures compatible with complex dynamical properties can be assembled by controlling the higher-order connectivity among the building blocks.

PACS numbers:

I. INTRODUCTION

Impact of the system's architecture onto emergent functionality in nanostructured materials has been evidenced by experimental investigation of the functional features by varying the building blocks in different self-assembly processes²⁻¹⁰. Theoretically, the structural elements that lead to an improved function can be identified by parallel investigations of the topology and dynamics of a particular system represented by nano-network¹¹, for example, by conducting nanoparticle films¹²⁻¹⁵, carbon nanotube fillers¹⁶, etc. On a more global scale, the interplay between the structure and dynamics is captured by spectral properties of networks^{17,18}. More specifically, spectral analysis of the adjacency matrix or the Laplacian operator related to the adjacency matrix¹⁹ revealed Fiedler spectral partitioning of the graph and detection of functional modules or mesoscopic communities^{20,21}, hierarchical organisation and homeostatic response²², the structural changes at the percolation threshold²³, or the occurrence of assortative correlations between nodes²⁴. A direct relation between the Laplacian eigenspectrum and the diffusion processes on that network revealed the role of the small-degree nodes and features of the return-time of random walks^{20,25}, as well as the universality of dynamical phase transitions²⁶ and a deeper understanding

of synchronisation on complex networks²⁷. In this context, the key quantity that relates the structure to the diffusion and synchronisation on a network is the *spectral dimension*²⁸⁻³⁰, which can be determined from the properties of the Laplacian spectrum.

The complex functional systems often exhibit a hierarchical architecture and the related hyperbolic geometry. They can be parameterised by *simplexes*, cliques of different orders, and described by mathematical techniques of the algebraic topology of graphs³¹⁻³⁵. In the materials science, such structures are grown by cooperative self-assembly^{2,6-10,36}. Moreover, the idea of hierarchical architecture is a center-piece in the development of many modern innovative technologies such as 3D printing³⁷. Recently, these processes have been modelled by attachments of pre-formatted objects under geometric constraints and specified binding rules^{1,5}. See other similar works in^{38,39}. Whereas, in real complex systems whose structure is detectable from experimental data, the corresponding networks can be decomposed into simplicial complexes. For example, in brain networks^{40,41} these simplicial complexes comprise the inner structure of brain anatomical modules. The hierarchical organisation was also found in social networking dynamics⁴²⁻⁴⁴, in problems related to traffic dynamics⁴⁵, and so on.

As mentioned above, the hierarchically organised net-

works possess emergent hyperbolicity or negative curvature in the shortest-path metric, that is they are Gromov hyperbolic graphs^{46–50}. Recently, the graphs with a small hyperbolicity parameter δ have been in the focus of the scientific community for their ubiquity in real systems and applications, as well as due to their mathematically interesting structure^{47–49,51}. Namely, the upper bound of a small hyperbolicity parameter can be determined from a subjacent smaller graph of a given structure. Generally, it is assumed that both naturally evolving, biological, physical and social systems develop a negative curvature to optimise their dynamics^{38,41,44,52,53}. However, the precise relationship between the hyperbolicity of a network and its spectral and dynamical features remains mostly unexplored.

In this paper, we tackle these issues by systematically analysing the spectral properties of a class of Gromov 1-hyperbolic networks but with the different architecture of simplicial complexes. Based on the model for the cooperative self-assembly of simplexes introduced in¹, here we grow several classes of nano-networks and analyse their topology and spectral properties; the monodisperse building blocks are cliques of the order $n = 3, 4, 5, 6$ while the geometrical compatibility tuns their assembly in the interplay with the varying chemical affinity ν of the growing structure towards the binding group. Specifically, for the negative values of the parameter ν , the effective repelling interaction between the simplexes occurs, while it is gradually attractive for the positive ν . At $\nu = 0$ purely geometrical factors play a role. Our results show that while the hyperbolicity parameter remains constant $\delta = 1$ for all classes, their spectral dimension varies with the chemical affinity ν and the size of the elementary building blocks n . Moreover, these networks exhibit a community structure when the parameter $\nu \geq 0$. The inner structure of these communities consists of simplicial complexes with a hierarchical architecture, which manifests itself in the characteristic spectral properties of the Laplacian of the network.

In Sec. II, we present details of the model and parameters, while in Sec. III we study different topology features of the considered networks. In Sec. IV we analyse in detail spectral properties of all classes of these networks for varied parameters ν and the size of elementary blocks. Sec. V is devoted to the discussion of the results.

II. SELF-ASSEMBLY OF SIMPLEXES AND THE TYPE OF EMERGENT STRUCTURES

To grow different nano-networks by chemical aggregation of simplexes, we apply the rules of the model for cooperative self-assembly^{1,54}. Pre-formatted groups of particles are described by simplexes (full graphs, cliques) of different size $n \equiv q_{max} + 1$, where q_{max} indicates the order of the clique. Starting from an initial simplex, at each step, a new simplex is added and attached to the growing network by *docking* along one of its faces,

which are recognised as simplexes of the lower order $q = 0, 1, 2, \dots, q_{max} - 1$, see online demo⁵⁵. For example, a tetrahedron can be attached by sharing a single nod, i.e., a simplex of the order $q = 0$ with the existing network, or sharing an edge, $q = 1$, or a triangle, $q = 2$, with an already existing simplex in the network. The attaching probability depends both on the geometrical compatibility of the q -face of the adding simplex with the current structure as well as on the parameter ν that describes the chemical affinity of that structure towards the addition of $n_a = q_{max} - q$ new vertices. More precisely, we have¹

$$p(q_{max}, q; t) = \frac{c_q(t)e^{-\nu(q_{max}-q)}}{\sum_{q=0}^{q_{max}-1} c_q(t)e^{-\nu(q_{max}-q)}} \quad (1)$$

for the normalised probability that a clique of the order q_{max} attaches along its face of the order q . Here, $c_q(t)$ is the number of the geometrically similar docking sites of the order q at the evolution time t . Eventually, one of them is selected randomly. By varying the parameter ν from large negative to large positive values, the probability of docking along with a particular face is considerably changed. For example, for the negative values of ν , the growing system 'likes' new vertices; consequently, a simplex preferably attaches along a shared vertex rather than a larger structure. Effectively, a repulsion between simplexes occurs, see Fig. 1 top. In the other limit, for a large positive ν , the most probable docking is along the potentially largest face, such that an added simplex of the size n shares the maximum number $n - 1$ of vertices with the existing structure, see bottom panel in Fig. 1 and Fig. 2. Here, the simplexes in question experience a strong attraction, which gradually decreases with decreasing ν . For the neutral case $\nu = 0$, the assembly is regulated by strictly geometrical compatibility factors $C_q(t)$, which change over time as the network grows.

In the original model¹, the size of the incoming simplexes is taken from a distribution, whose parameters can be varied. To reveal the impact of the size of these building blocks on the spectral properties of the new structure, here we focus on the networks with *monodisperse* cliques, in particular, we investigate separately the structures grown by aggregation of cliques of the size $n = 3, 4, 5$ and 6 for varied affinity ν . For comparison, we also consider the case with a distribution of simplexes in the range $n \in [3, 6]$. As the examples in Fig. 1 and Fig. 2 show, the structure of the assembly varies considerably both with the size of simplexes and the level of attraction between them. Notice that in the case $n = 2$ the simplex consists of two vertices with an edge between them resulting in a simple random tree graph. Here, $q_{max} = 1$ and all docking faces are single-vertex sites ($q = 0$). Therefore, the probability $p(1, 0; t) = 1$ is independent of the value of the parameter ν . In this work, we consider networks of different number of vertices $N = 1000, 5000, \text{ and } 10000$.



FIG. 1: Aggregates of tetrahedra with strong repulsion, a segment is shown in the top panel, and the case with strong attraction resulting in the network with communities is shown in the bottom panel.

III. TOPOLOGICAL PROPERTIES OF THE ASSEMBLED NANO-NETWORKS

The structure of the assemblies strongly depends on the chemical affinity ν and the size n of the building blocks. For example, a strong repulsion between cliques enables sharing a single node, thus minimising the geometrical compatibility factor and resulting in a sparse graph (a tree-of-cliques). An example with the tetrahedra as building blocks at $\nu = -9$ is shown in the top panel of Fig. 1. However, for extremally attractive cliques, e.g., for $\nu = 9$, the same building blocks attach mostly via sharing their largest subgraphs (triangles); thus the geometrical constraints play an important role. This situation results in a dense network with a nontrivial community structure, as shown in the bottom panel of Fig. 1 and Fig. 2. Meanwhile, the modules in the sparse structure can be recognised as the elementary cliques. Notably, the presence of a large clique increases the efficiency of building a nontrivial structure, even for a small attractive potential, cf. Fig. 2 top. We will further discuss the community structure of these networks in connection with their spectral properties in Sec. IV. In Table I we show different graph measures of some mono-disperse assemblies whose spectral properties are studied in Sec. IV. We note that the self-assembly process of cliques can result in a broad range of the degree of vertices. Depending on the size of cliques $n \geq 3$, several hubs and a power-

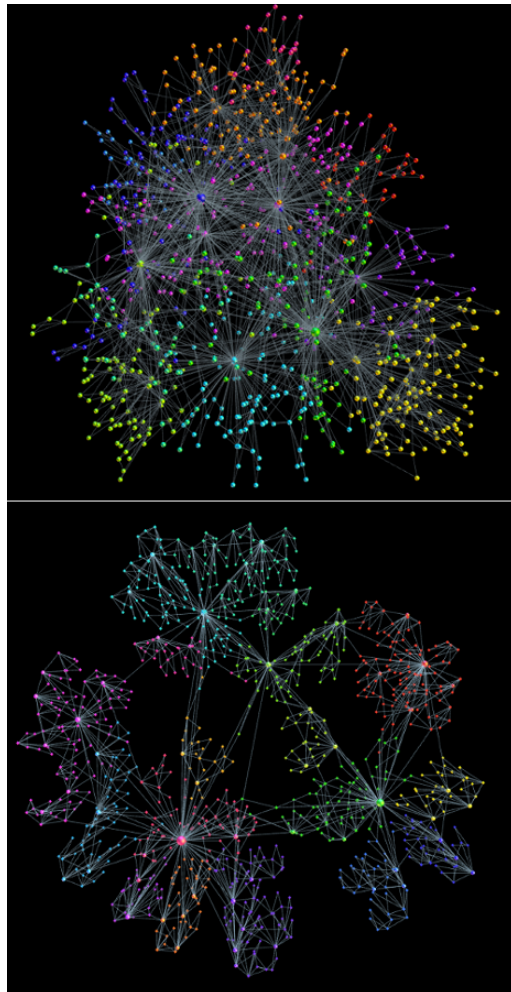


FIG. 2: The networks of the aggregated cliques of mixed sizes $n \in [3, 6]$ distributed according to $\propto n^{-2}$ for $\nu = 5$ (top), and aggregates of triangles for $\nu = 9$ (bottom). The community structure is indicated by different colours of nodes.

law tail can appear at the sufficiently strong attraction between them¹. For illustration, Fig. 3 shows the ranking distribution of the degree for several monodisperse assemblies in the case of strong attraction.

As mentioned above, the assemblies of cliques possess a negative curvature in the graph metric space, which implies that they fulfil the Gromov 4-point hyperbolicity criterion⁴⁶. More precisely, the graph G is hyperbolic *iff* there is a constant $\delta(G)$ such that for any four vertices (a, b, c, d) , the relation $d(a, b) + d(c, d) \leq d(a, d) + d(b, c) \leq d(a, c) + d(b, d)$ implies that

$$\delta(a, b, c, d) = \frac{d(a, c) + d(b, d) - d(a, d) - d(b, c)}{2} \leq \delta(G), \quad (2)$$

where $d(u, v)$ indicates the shortest path distance. Note that the difference in (2) is bounded from above by the minimum distance in the smallest sum $d_{min} \equiv \min\{d(a, b), d(c, d)\}$. Thus, by plotting $\delta(a, b, c, d)$ against d_{min} for a large number of 4-tuples, we numer-

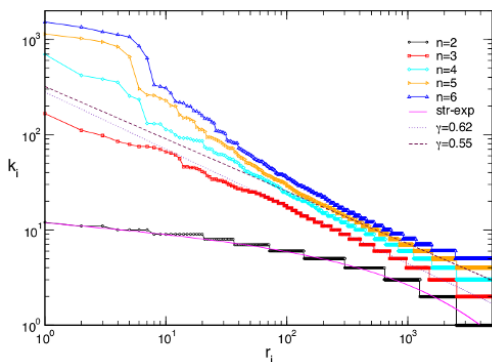


FIG. 3: The degree k_i of the vertex i plotted against the vertex rank r_i for different assemblies of cliques of size n , indicated in the legend, and $\nu = 9$. Stretched exponential curve approximates the data for the random tree ($n = 2$), while the asymptotic power-law decay with the exponent γ is appropriate for $n \geq 3$.

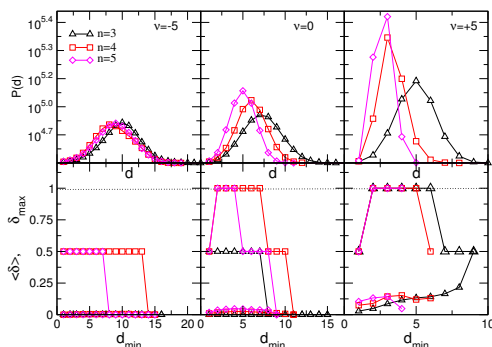


FIG. 4: Shortest-path distance distributions $P(d)$ vs the distance d and hyperbolicity parameter δ_{max} and $\langle d \rangle$ vs d_{min} for the assemblies of simplexes indicated in the legend, and three distinct values of the chemical affinity parameter ν .

ically estimate $\delta(G) \equiv \delta_{max}$ as the maximum value observed in the entire graph.

As described in Sec. II, the cliques aggregate by sharing their faces, i.e., cliques of a lower order, which leads to some specific properties of the grown structures¹. In particular, the order of the simplicial complex cannot exceed the order of the largest attaching clique. Moreover, theoretical investigations of these types of structures predict^{47–50} that the upper bound of the hyperbolicity parameter of the graph differs from the hyperbolicity of the "atoms" of the structure by at most one unit, that is $\delta_{max} = \delta_a + 1$. Given that a clique is ideally hyperbolic (i.e., tree-like in the shortest path metric space), we have $\delta_a = 0$, which gives $\delta_{max} = 1$ for all clique complexes grown by the rules of our model. By sampling up to 10^9 4-tuples of vertices and computing the graph hyperbolicity parameter $\delta(G)$ in Eq. (2), we demonstrate that the hyperbolicity parameter remains $\delta(G) \leq 1$ for all studied assemblies. More precisely, while the structure of different assemblies, as well as their distribution of the

TABLE I: Graph measures of the assemblies of cliques of the size n with $N \approx 1000$ vertices for three representative values of the affinity parameter ν : The number of edges E , average degree $\langle k \rangle$ and clustering coefficient $\langle Cc \rangle$, graph's modularity mod , diameter D and the ratio of the hyperbolicity parameter δ_{max} to $D/2$. Two bottom rows are for mixed clique sizes $n \in [3, 6]$ distributed according to $\propto n^{-\alpha}$.

| bb | ν | E | $\langle k \rangle$ | $\langle Cc \rangle$ | $\langle \ell \rangle$ | mod | D | $\delta_{max}/D/2$ |
|--------------|-------|------|---------------------|----------------------|------------------------|-------|----|--------------------|
| $n = 3$ | -5 | 1501 | 2.999 | 0.766 | 9.789 | 0.928 | 22 | 1/11 |
| | 0 | 1734 | 3.465 | 0.741 | 7.265 | 0.902 | 16 | 1/8 |
| | +5 | 1991 | 3.982 | 0.735 | 4.958 | 0.861 | 10 | 1/5 |
| $n = 4$ | -5 | 2009 | 4.61 | 0.847 | 8.718 | 0.927 | 19 | 2/19 |
| | 0 | 2426 | 4.852 | 0.808 | 6.023 | 0.895 | 12 | 1/6 |
| | +5 | 2984 | 5.968 | 0.813 | 3.23 | 0.715 | 8 | 1/4 |
| $n = 5$ | -5 | 2514 | 5.013 | 0.878 | 8.89 | 0.921 | 19 | 2/19 |
| | 0 | 3182 | 6.351 | 0.829 | 5.01 | 0.856 | 11 | 2/11 |
| | +5 | 3997 | 7.958 | 0.850 | 2.703 | 0.850 | 5 | 2/5 |
| $\alpha = 2$ | +5 | 2905 | 5.810 | 0.820 | 3.172 | 0.620 | 7 | 2/7 |
| $\alpha = 0$ | +5 | 3464 | 6.298 | 0.844 | 2.857 | 0.569 | 6 | 1/3 |

shortest-path distances, vary with the chemical affinity ν , the upper bound of their hyperbolicity parameter remains fixed in agreement with the theoretical prediction. In Fig. 4, we show the results of the numerical analysis for three representative sets of the assemblies of cliques of different sizes. See also Table I.

IV. SPECTRAL ANALYSIS OF MONODISPERSE ASSEMBLIES

Spectral dimension d_s of a graph, which is defined via $\lim_{t \rightarrow \infty} \frac{\log P_{ii}(t)}{\log t} = -\frac{d_s}{2}$, characterises the distribution of return time $P_{ii}(t)$ of a random walk on that graph^{28,56–58}. The diffusion type of processes on network are described by Laplacian operators^{20,25}. More precisely, for the undirected graph of N vertices, two types of diffusion operators are defined, i.e., the Laplacian operator with the components

$$L_{ij} = k_i \delta_{ij} - A_{ij}, \quad (3)$$

and the symmetric normalised Laplacian⁵⁹

$$L_{ij}^n = \delta_{ij} - \frac{A_{ij}}{\sqrt{k_i k_j}}. \quad (4)$$

Here, A_{ij} are the matrix elements of the adjacency matrix, k_i is the degree of the node i , and δ_{ij} is the Kronecker symbol. The operators defined with Eq. (3) and (4) are symmetric and have real non-negative eigenvalues. Both operators have the eigenvalue $\lambda = 0$ with the degeneracy that is equal to the number of connected components in the network. For the networks that have a finite spectral dimension, spectral densities of both Laplacians scale as $P(\lambda) \simeq \lambda^{\frac{d_s}{2}-1}$ for small values of λ . Therefore, the corresponding cumulative distribution $P_c(\lambda)$ scales as

$$P_c(\lambda) \simeq \lambda^{\frac{d_s}{2}}, \quad \lambda \ll 1 \quad (5)$$

and it is suitable³⁰ for estimating the spectral dimension d_s of the network. Here, we analyse the spectral properties of both Laplacian operators (3) and (4) for the networks grown with different building blocks and varied chemical affinity ν , see Figures 5-7.

We analyse the cumulative spectral density $P_c(\lambda)$ for the Laplacian defined by the expression (3) to determine the spectral dimension of the graphs with the adjacency matrix A_{ij} . Note that the spectrum is bounded from below, i.e., $0 \leq \lambda$ for all eigenvalues λ . According to Eq. (5), we estimate d_s for each sample by fitting the data of $P_c(\lambda)$ for the values in the range $\lambda \lesssim 0.3$, as illustrated in Fig. 6. The error bars are determined by taking the average from different samples of networks that have 1000 and 5000 nodes. The results summarised in Fig. (5) show how the spectral dimension of the corresponding graphs varies with the chemical affinity ν depending on the size of the elementary building blocks.

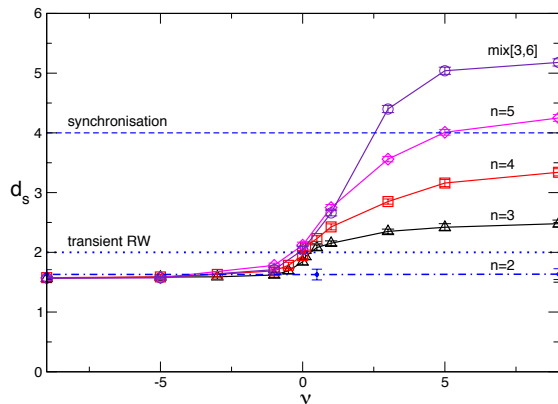


FIG. 5: The lines with different symbols represent the spectral dimension d_s plotted against chemical affinity ν for the aggregates of monodisperse cliques of sizes $n = 3, 4, 5$ and a mixture of cliques of different sizes in the range $n \in [3, 6]$. The bottom line corresponds to the random tree case $n = 2$.

As Fig. 5 shows, the impact of the size of the cliques strongly depends on the way that they aggregate, which is controlled by the chemical affinity ν . Precisely, for the sparse structures grown under the considerable repulsion between cliques when $\nu < 0$, we find that the spectral dimension is practically independent of the size of cliques until the repulsion becomes vanishingly weak. In contrast, when $\nu \geq 0$ the spectral dimension increases with the size of the elementary cliques. Here, the attaching cliques can share their larger faces thus increasing the impact of the geometrical compatibility factor. Remarkably, the spectral dimension increases with the strength of the attraction between cliques, which favours sharing increasingly larger faces. These faces are limited by the size of the elementary cliques. More specifically, for all $\nu \geq 0$ values, d_s is systematically larger in the aggregates of tetrahedra than those of triangles. In both cases we have that d_s exceeds the limit of the transient random walk, $d_s = 2$, for relatively weak attraction be-

tween cliques $\nu \sim 1$. However, both curves remain below $d_s = 4$ for the entire range of ν values. Note that $d_s > 4$ is recognised as the full synchronisation condition for the Kuramoto oscillators on network³⁰. Whereas, in the region $d_s \in (2, 4]$ an entrained synchronisation with a complex spatio-temporal patterns can be expected^{30,60}. Even though a quite compact structure is grown by attaching tetrahedrons via their triangular faces, see bottom panel in Fig. 1, its spectral dimension remains limited as $d_s < 4$, enabling the complex synchronisation patterns. We find that the limit $d_s = 4$, can be exceeded when the size of the clique is at least $n = 5$ and the attraction is considerably large, i.e., $\nu \geq 5$. In this situation, the agglomerate consists of 5-cliques sharing many tetrahedrons as their largest faces. Interestingly, it suffices to have a few cliques of a large size to grow such agglomerates that cause the spectral dimension $d_s \geq 4$. For example, the mixture shown in the top panel of Fig. 2 with $n \in [3, 6]$, where the population of 6-cliques is only 1/4 of the population of 3-cliques, leads to the spectral dimension shown by the top line in Fig. 5. Furthermore, Fig. 6 indicates that not only the spectral dimension but the entire spectrum changes with the size of the cliques and the chemical affinity, as we discuss in more detail in the following.

Next, we determine the spectral density of the normalised Laplacian, defined by (4), by averaging over 10 networks of size $N \approx 1000$ generated for the same values of the model parameters. Note that the eigenvalues of the normalised Laplacian are bounded in the range^{20,25} $\lambda_{LN} \in [0, 2]$. In Fig. 7, we show the spectral density of the normalised Laplacian for several representative cases, in particular, for three different aggregates of tetrahedrons corresponding to the strong repulsion, vanishing interaction, and strong attraction, respectively. Besides, in the panel (c), the spectral distribution is shown for the case of strong attraction $\nu = 9$ for the cliques of different sizes $n \geq 3$. It should be noted that iso-spectral structures are observed in the case of the significant repulsion between the cliques $\nu = -9$. In this limit, apart from a structure at small eigenvalues, there is a prominent peak at $\lambda_{LN} = n/(n-1)$, indicating the presence of minimally connected cliques. In contrast, for $\nu \geq 0$, the attraction between cliques and the relevance of the geometrical compatibility factors lead to the appearance of larger simplicial complexes. A peak starts building at $\lambda_{LN} = 1$ already at $\nu = 0$, which gradually increases with the increasing ν , as shown in the panel (c). The occurrence of the peak at $\lambda_{LN} = 1$, (i.e., $\lambda = 0$ in the corresponding adjacency matrix¹⁹) appears as a characteristic feature of these hyperbolic networks. According to previous studies of scale-free and modular networks^{20,25}, this peak is related to the nodes of the lowest degrees in the network.

In the present study, such nodes are found in the bottom-right corner of the ranking distribution in Fig. 3. Apart from the random tree case, the appearance of this peak reflects the fact that with the increased

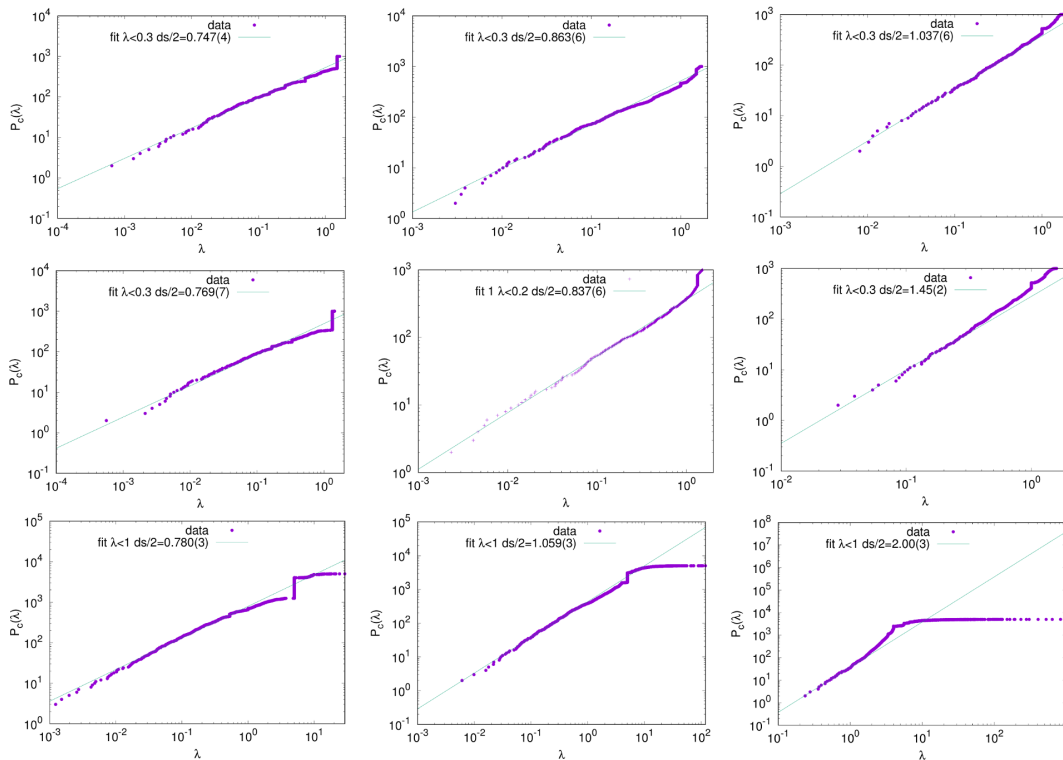


FIG. 6: Several examples of the cumulative spectral density $P_c(\lambda)$ in the range of small λ for the Laplacian operator (3) for the aggregates of triangles (top row), tetrahedra (middle row) and 5-cliques (bottom row) for varied chemical affinity $\nu = -5, 0,$ and $+5$, left-to-right column.

chemical affinity a broad distribution of degrees occurs with a power-law tail, cf. Fig. 3. Notably, the highest peak is when the building cliques are of different sizes $n \in [3, 6]$, compared to the monodisperse structure with $n = 6$. A further exciting feature of these spectral densities is that a characteristic minimum appears between $\lambda_{LN} = 1$ and the structure above it. The results in previous investigations²² suggest that such minimum in the spectral density is a signature of the hierarchically organised network. In the present study, the hierarchical organisation of cliques into simplicial complexes occurring at $\nu \geq 0$ has been demonstrated by the algebraic topology methods in¹. Here, we show by the spectral analysis that these simplicial complexes make the inner structure of mesoscopic communities, which can be identified by the localisation of the eigenvectors of the lowest non-zero eigenvalues²⁰. In the right column of Fig. 7, we show the scatter plot of the three eigenvectors related to the lowest nonzero eigenvalues corresponding to the aggregates of tetrahedrons in the left column. In the limit of strong repulsion between the cliques, the modularity of the entire structure is determined by the original cliques, see top right panel of Fig. 7. Whereas, the larger communities with sub-communities appear for $\nu \geq 0$ where higher-order connections are increasingly more effective, cf. panels (b1) and (c1) of Fig. 7. The bottom panel corresponds to the random tree structure ($n = 2$).

V. DISCUSSION AND CONCLUSIONS

We have studied topological and spectral properties of classes of hyperbolic nano-networks grown by the cooperative self-assembly. The growth rules¹ that can be tuned by changing the parameter of chemical affinity ν enable to investigate the role of higher-order connectivity in the properties of the emerging structure. Attaching groups of particles are parameterised by simplexes (cliques) of different sizes which share a geometrical sub-structure by docking along with the growing network. For the negative values $\nu < 0$, the repulsion among cliques makes them share a single node rather than an edge or a higher structure. On the other hand, $\nu \geq 0$ implies that the geometrical factors and the size of the attaching clique become relevant. In particular, the higher positive value of ν implies that a new clique attaches to a previously added clique by sharing its face of the larger order, thus building a more compact structure. Mathematically⁵⁰, the attachment of cliques by sharing a face (of any order) leads to simplicial complexes whose hyperbolicity parameter cannot exceed one.

Our results revealed that, while the hyperbolicity parameter remains fixed $\delta_{max} = 1$ across different assemblies, their topological and spectral properties change with the increased chemical affinity, see Table I and Fig. 5 and Fig. 7. Remarkably, the spectral dimension of the

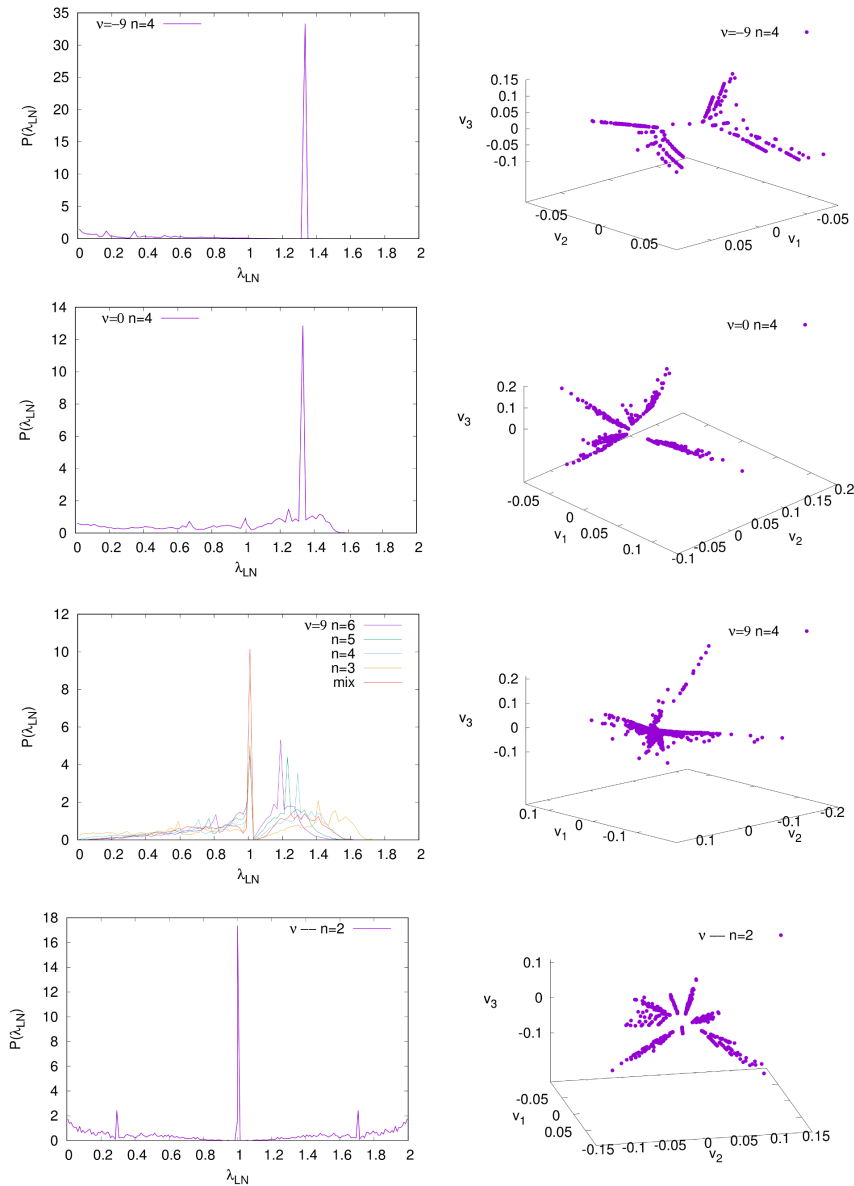


FIG. 7: Spectral distribution (left column) and the corresponding scatter plots of the eigenvectors of the lowest nonzero eigenvalues of the normalized Laplacian (right column) for the aggregates of tetrahedra (a-c,a1-c1) for $\nu = -9, 0$, and $+9$, and for the random tree structure $n = 2$, which is independent of ν , (d,d1).

structure of strongly-repelled cliques of any size is practically indistinguishable from the one of a random tree of the same number of vertices. However, the rest of the spectrum is different from the one of the tree structure; its dominant feature is the presence of cliques as the prominent network modules. On the other hand, the compelling attraction between the cliques for $\nu \gtrsim 0$ results in the spectral dimension that for all sizes $n \geq 3$ exceeds the limit $d_s = 2$, compatible with the transient random walk on the network. Further increase of the spectral dimension with the increased affinity parameter ν strongly depends on the size of the cliques. Our results suggest that for a strong attraction with the cliques of

size $n \geq 5$, the spectral dimension of the network can exceed the limit $d_s = 4$, above which the synchronised phase is expected to exist³⁰. However, more interesting structures are grown by smaller cliques or a mixture of different clique sizes with a weak attraction (small positive values of the parameter ν) allowing the sharing a variety of clique's faces. In these cases, we find that the spectral dimension remains in the range of $d_s \in (2, 4]$. These spectral properties are expected to be compatible with an entrained synchronisation³⁰ or a frustrated hierarchical synchronisation with intricate spatiotemporal patterns⁶⁰. A detailed analysis of such synchronisation patterns on these graphs as well as potentially super-

diffusive processes⁶¹ remains for future work. Due to their spectral properties, these structures can be interesting for modelling the complex dynamics in a variety of biological systems and for potential applications. In the framework of the cooperative self-assembly of nanoparticle groups, our analysis shows how the control of the chemical affinity can lead to complex structures with different functional properties. Furthermore, the presented results can be relevant for a deeper understanding of the functional complexity of many important structures with built-in simplicial complexes, such as human connectome⁴¹ and other hierarchically modular networks.

Acknowledgments

The authors acknowledge the financial support from the Slovenian Research Agency (research code funding number P1-0044) and from the Ministry of Education, Science and Technological Development of the Republic of Serbia, the Projects ON171017 and by the Ito Foundation fellowship.

-
- ¹ [I] M. Šuvakov, M. Andjelković, and B. Tadić. Hidden geometries in networks arising from cooperative self-assembly. *Scientific Reports*, 8:1987–1–10 (2018).
- ² M. A. Boles, M. Engel, and D. V. Talapin. Self-assembly of colloidal nanocrystals: From intricate structures to functional materials. *Chemical Reviews*, 116(18):11220–11289 (2016). PMID: 27552640.
- ³ D. Toulemon, M.V. Rastei, D. Schmool, J.S. Garitaonandia, L. Lezama, X. Cattoen, S. Begin-Collin, and B.P. Pichon. Enhanced collective magnetic properties induced by the controlled assembly of iron oxide nanoparticles in chains. *Adv. Funct. Mat.*, 26(15):1616–3028 (2016).
- ⁴ A. Hirata, L. J. Kang, T. Fujita, B. Klumov, K. Matsue, M. Kotani, A. R. Yavari, and M. W. Chen. Geometric frustration of icosahedron in metallic glasses. *Science*, 7(10):1232450 (2013).
- ⁵ S. Ikeda and M. Kotani. Materials inspired by mathematics. *Science and Technology of Advanced Materials*, 17(1):253–259 (2016).
- ⁶ D. Luo, C. Yan, and T. Wang. Interparticle forces underlying nanoparticle self-assemblies. *Small*, 11(45):5984–6008 (2015).
- ⁷ S. Liu and J. Yu. Cooperative self-construction and enhanced optical absorption of nanoplates-assembled hierarchical Bi₂WO₆ flowers. *Journal of Solid State Chemistry*, 181(5):1048 – 1055 (2008).
- ⁸ C. J. Meledandri, J. K. Stolarczyk, and D. F. Brougham. Hierarchical gold-decorated magnetic nanoparticle clusters with controlled size. *ACS Nano*, 5(3):1747–1755 (2011).
- ⁹ Y. Gu, R. Burtovyy, J. Townsend, J. R. Owens, I. Luzinov, and K. G. Kornev. Collective alignment of nanorods in thin newtonian films. *Soft Matter*, 9:8532–8539 (2013).
- ¹⁰ B. Senyuk, Q. Liu, E. Bililign, P. D. Nystrom, and I. I. Smalyukh. Geometry-guided colloidal interactions and self-tiling of elastic dipoles formed by truncated pyramid particles in liquid crystals. *Phys. Rev. E*, 91:040501 (2015).
- ¹¹ J. Živković and B. Tadić. Nanonetworks: The graph theory framework for modeling nanoscale systems. *Nanoscale Systems MMTA*, 2:30–48 (2013).
- ¹² M. O. Blunt, M. Šuvakov, F. Pulizzi, C. P. Martin, E. Pauliac-Vaujour, A. Stannard, A. W. Rushforth, B. Tadić, and P. Moriarty. Charge transport in cellular nanoparticle networks: meandering through nanoscale mazes. *Nano Letters*, 7(4):855–860 (2007).
- ¹³ M. Šuvakov and B. Tadić. Modeling collective charge transport in nanoparticle assemblies. *Journal of Physics: Condensed Matter*, 22(16):163201 (2010).
- ¹⁴ M. Šuvakov and B. Tadić. Transport processes on homogeneous planar graphs with scale-free loops. *Physica A: Statistical Mechanics and its Applications*, 372(2):354 – 361 (2006). Nonlinearity, Nonequilibrium and Complexity: Questions and Perspectives in Statistical Physics.
- ¹⁵ B. Tadić, M. Andjelković, and M. Šuvakov. The influence of architecture of nanoparticle networks on collective charge transport revealed by the fractal time series and topology of phase space manifolds. *Journal of Coupled Systems and Multiscale Dynamics*, 4(1):30–42 (2016).
- ¹⁶ Weng, G.-M. et al, Layer-by-Layer Assembly of Cross-Functional Semi-transparent MXene-Carbon Nanotubes Composite Films for Next-Generation Electromagnetic Interference Shielding. *Advanced Funct. Materials*, 28(44):1803360 (2018).
- ¹⁷ C. Castellano and R. Pastor-Satorras. Relating topological determinants of complex networks to their spectral properties: Structural and dynamical effects. *Phys. Rev. X*, 7:041024 (2017).
- ¹⁸ C. Sarkar and S. Jalan. Spectral properties of complex networks. *Chaos: An Interdisciplinary Journal of Nonlinear Science*, 28:102101 (2018).
- ¹⁹ J.F. Lutzeyer and A.T. Walden. Comparing Graph Spectra of Adjacency and Laplacian Matrices. *arXiv preprint arXiv:1712.03769* (2017).
- ²⁰ M. Mitrović and B. Tadić. Spectral and dynamical properties in classes of sparse networks with mesoscopic inhomogeneities. *Phys. Rev. E*, 80:026123 (2009).
- ²¹ E. Andreotti, D. Remondini, G. Servizi, and A. Bazzani. On the multiplicity of laplacian eigenvalues and fiedler partitions. *Linear Algebra and its Applications*, 544:206 – 222 (2018).
- ²² M. A. M. de Aguiar and Y. Bar-Yam. Spectral analysis and the dynamic response of complex networks. *Phys. Rev. E*, 71:016106 (2005).
- ²³ G. Palla and G. Vattay. Spectral transitions in networks. *New Journal of Physics*, 8(12):307 (2006).
- ²⁴ S. Jalan and A. Yadav. Assortative and disassortative mixing investigated using the spectra of graphs. *Phys. Rev. E*, 91:012813 (2015).
- ²⁵ S. N. Dorogovtsev, A. V. Goltsev, J. F. F. Mendes, and A. N. Samukhin. Spectra of complex networks. *Phys. Rev. E*, 68:046109 (2003).
- ²⁶ O. Shpielberg, T. Nemoto, and J. Caetano. Universality in dynamical phase transitions of diffusive systems. *Phys.*

- Rev. E*, 98:052116 (2018).
- 27 A. Arenas, A. Díaz-Guilera, J. Kurths, Y. Moreno, and C. Zhou. Synchronization in complex networks. *Physics Reports*, 469(3):93 – 153 (2008).
 - 28 B. Durhuus, T. Jonsson, and J. F. Wheeler. The spectral dimension of generic trees. *Journal of Statistical Physics*, 128(5):1237–1260 (2007).
 - 29 I. Seroussi and N. Sochen. Spectral analysis of a non-equilibrium stochastic dynamics on a general network. *Scientific Reports*, 8:14333 (2018).
 - 30 A. P. Millán, J. J. Torres, and G. Bianconi. Synchronization in network geometries with finite spectral dimension. *Physical Review E*, 99(2):022307 (2019).
 - 31 R.H. Atkin. From cohomology in physics to q-connectivity in social science. *International Journal of Man-Machine Studies*, 4(2):139 – 167 (1972).
 - 32 P. Gould. Q-analysis, or a language of structure: an introduction for social scientists, geographers and planners. *International Journal of Man-Machine Studies*, 13(2):169 – 199 (1980).
 - 33 H.-J. Bandelt and V. Chepoi. Metric graph theory and geometry: a survey, in Goodman, J. E.; Pach, J.; Pollack, R., eds. "Surveys on discrete and computational geometry: Twenty years later". volume 453. Providence, RI: AMS, 2008.
 - 34 Jonsson J. *Simplicial Complexes of Graphs*. Lecture Notes in Mathematics, Springer-Verlag, Berlin, 2008.
 - 35 S. Maletić and Y. Zhao. *Simplicial Complexes in Complex Systems: The Search for Alternatives*. Harbin Institute of Technology, Harbin, Peoples Republic of China, first edition, 2017.
 - 36 D. Toulémon, M. V. Rastei, D. Schmool, J. S. Garitanoandia, L. Lezama, X. Catton, S. Bgin-Colin, and B. P. Pichon. Enhanced collective magnetic properties induced by the controlled assembly of iron oxide nanoparticles in chains. *Advanced Functional Materials*, 26(15):2454–2462 (2016).
 - 37 J.U. Surjadi, L. Gao, H. Du, X. Li, X. Xiong, N. X. Fang, Y. Lu. Mechanical Metamaterials and Their Engineering Applications. *ADVANCED ENGINEERING MATERIALS*, 21(3): 1800864 (2019).
 - 38 G. Bianconi and C. Rahmede. Emergent hyperbolic network geometry. *Sci. Rep.*, 7:41974 (2017).
 - 39 N. Cinardi, A. Rapisarda, and G. Bianconi. Quantum statistics in network geometry with fractional flavor. *arXiv:1902.10035v1*, pages 1–60 (2019).
 - 40 B. Tadić, M. Andjelković, B. M. Boshkoska, and Z. Levnajić. Algebraic topology of multi-brain connectivity networks reveals dissimilarity in functional patterns during spoken communications. *PLOS ONE*, 11(11):1–25 (2016).
 - 41 B. Tadić, M. Andjelković, and R. Melnik. Functional geometry of human connectome and robustness of gender differences. *arXiv:1904.03399 [q-bio.NC]* (2019).
 - 42 M. Andjelković, B. Tadić, S. Maletić, and M. Rajković. Hierarchical sequencing of online social graphs. *Physica A: Statistical Mechanics and its Applications*, 436:582 – 595 (2015).
 - 43 M. Andjelković, B. Tadić, M. Mitrović Dankulov, M. Rajković, and R. Melnik. Topology of innovation spaces in the knowledge networks emerging through questions-and-answers. *PLOS ONE*, 11(5):1–17 (2016).
 - 44 Bosiljka Tadić. Self-organised criticality and emergent hyperbolic networks: blueprint for complexity in social dynamics. *European Journal of Physics*, 40(2):024002 (2019).
 - 45 M. Andjelković, N. Gupte, and B. Tadić. Hidden geometry of traffic jamming. *Phys. Rev. E*, 91:052817 (2015).
 - 46 J.M. Rodriguez and E. Touris. Gromov hyperbolicity through decomposition of metric spaces. *Acta Math. Hungar.*, 103:53–84 (2004).
 - 47 S. Bermudo, J. M. Rodríguez, J. M. Sigarreta, and J.-M. Vilaire. Gromov hyperbolic graphs. *Discrete Mathematics*, 313(15):1575 – 1585 (2013).
 - 48 S. Bermudo, J. M. Rodríguez, O. Rosario, and J. M. Sigarreta. Small values of the hyperbolicity constant in graphs. *Discrete Mathematics*, 339(12):3073 – 3084 (2016).
 - 49 A. Martinez-Perez. Generalized chordality, vertex separators and hyperbolicity on graphs. *arXiv:1708.06153v1*, pages 1–16 (2017).
 - 50 N. Cohen, D. Coudert, G. Ducoffe, and A. Lancin. Applying clique-decomposition for computing gromov hyperbolicity. *Theoretical Computer Science*, 690(Supplement C):114 – 139 (2017).
 - 51 W. Carballosa, D. Pestana, J. M. Rodríguez, and J. M. Sigarreta. Distortion of the hyperbolicity constant in minor graphs. *Electronic Notes in Discrete Mathematics*, 46:57 – 64 (2014). Jornadas de Matemática Discreta y Algoritmica.
 - 52 W. S. Kennedy, I. Saniee, and O. Narayan. On the hyperbolicity of large-scale networks and its estimation. In *2016 IEEE International Conference on Big Data (Big Data)*, pp. 3344–3351 (2016).
 - 53 V. Salnikov, D. Cassese, and R. Lambiotte. Simplicial complexes and complex systems. *arXiv:1807.07747*, (2018).
 - 54 M. Šuvakov and B. Tadić. *Topology of Cell-Aggregated Planar Graphs*, pp. 1098–1105. Springer Berlin Heidelberg, Berlin, Heidelberg, 2006.
 - 55 M. Šuvakov, M. Andjelković, and B. Tadić. Applet: Simplex aggregated growing graph (<http://suki.ipb.rs/ggraph/>). 2017.
 - 56 R. Rammal and G. Toulouse. Random walks on fractal structures and percolation clusters. *Journal de Physique Lettres*, 44(1):13–22 (1983).
 - 57 R. Burioni and D. Cassi. Universal properties of spectral dimension. *Physical review letters*, 76(7):1091 (1996).
 - 58 R. Burioni and D. Cassi. Random walks on graphs: ideas, techniques and results. *Journal of Physics A: Mathematical and General*, 38(8):R45 (2005).
 - 59 A. N. Samukhin, S. N. Dorogovtsev, and J. F. F. Mendes. Laplacian spectra of, and random walks on, complex networks: Are scale-free architectures really important? *Phys. Rev. E*, 77:036115 (2008).
 - 60 P. Villegas, P. Moretti, and M.A. Muñoz. Frustrated hierarchical synchronization and emergent complexity in the human connectome network. *Sci. Rep.*, 4:5990 (2014).
 - 61 B. Tadić and S. Thurner. Information superdiffusion on structured networks. *Physica A: Statistical Mechanics and its Applications* 332, 566-584 (2004).